Microbial Ecology (2026) 89:26
https://doi.org/10.1007/s00248-025-02673-3

RESEARCH

Contrasting Nitrogen Fixation Between Arctic and Atlantic Waters in the Fram Strait

Stine Zander[1] · Lisa W. von Friesen[1,7] · Rafael Gonçalves-Araujo[2] · Olivier Grosso[3] · Mar Benavides[3,4,5] · Mats A. Granskog[6] · Lasse Riemann[1]

Received: 15 September 2025 / Accepted: 26 November 2025

Abstract

Nitrogen availability limits primary production in the Arctic Ocean, making it vital to understand its sources and sinks to predict future productivity. Although nitrogen fixation has been reported in the Arctic Ocean, data remain scarce, especially in the Atlantic sector. Here, we measured nitrogen fixation rates and examined diazotroph community composition across the Fram Strait, targeting Polar waters in the East Greenland Current, Atlantic waters in the West Spitsbergen Current, and their frontal zone. Nitrogen fixation was mainly low (< 1 nmol N L^{-1} d^{-1}) in Polar waters, however, elevated at the one station in the Atlantic water sector (up to 10.15 nmol N L^{-1} d^{-1}). Rates were only detectable in the epipelagic layer (0–100 m) across the strait and positively correlated with temperature, primary production, and chlorophyll-*a* fluorescence, and negatively correlated with coloured dissolved organic matter and silicate. The diazotrophs were dominated by non-cyanobacterial diazotrophs (NCDs; 77% of *nifH* amplicon reads), with an Arctic Betaproteobacterial group (order *Rhodocyclales*) accounting for 11% of sequence reads. This group was quantifiable (up to 6700 *nifH* gene copies L^{-1}) within the West Spitsbergen Current and the frontal zone, where the highest nitrogen fixation and primary production occurred, and its prevalence was positively correlated with temperature. We propose that temperature and freshly produced dissolved organic matter influence the NCD-dominated nitrogen fixation in Fram Strait. Our study suggests that NCDs are key diazotrophs in Fram Strait, and that nitrogen fixation rates and their potential importance for primary production vary across the contrasting water masses entering and exiting the Arctic Ocean. We encourage future studies to quantify these nitrogen fluxes and evaluate their importance for productivity in the Arctic Ocean.

Keywords NifH · Non-cyanobacterial diazotrophs · Stable isotope tracing

Introduction

Although being the smallest ocean on Earth, the Arctic Ocean (AO) accounts for up to 14% of the global marine net annual CO_2 uptake [1, 2]. The Arctic is warming up to four times faster than the global average, resulting in profound environmental changes [3, 4]. One distinct consequence is the reduction in sea ice [5], causing stimulation of primary production due to increased light availability and longer growth seasons [6–9]. As a response to sea ice reduction, nitrogen (N) availability, which commonly limits primary production in the AO [10, 11], is predicted to decrease [12]. In addition to sea ice decline, the warming is enhancing "Atlantification", seen as an increased inflow of warm, saline Atlantic water to the AO, causing changes in e.g., stratification, species composition, and nutrient concentrations [13, 14]. Consequently, improving our understanding

✉ Lasse Riemann
lriemann@bio.ku.dk

1 Marine Biological Section, Department of Biology, University of Copenhagen, Helsingør, Denmark

2 National Institute of Aquatic Resources, Technical University of Denmark, Kgs. Lyngby, Denmark

3 Aix Marseille University, Université de Toulon, CNRS, IRD, MIO UM 110, Marseille 13288, France

4 Turing Centre for Living Systems, Aix-Marseille University, Marseille 13009, France

5 National Oceanography Centre, European Way, Southampton SO14 3ZH, United Kingdom

6 Norwegian Polar Institute, Fram Centre, Tromsø 9296, Norway

7 Present address: Centre for Ecology and Evolution in Microbial Model Systems (EEMiS), Linnaeus University, Kalmar 39231, Sweden

Published online: 16 December 2025

of N sources is important for predictions of future nutrient availability, primary production, carbon sequestration, and ecosystem productivity in the AO.

Nitrogen fixation is a process carried out by specific microorganisms termed diazotrophs. It converts inert dinitrogen (N_2) gas to bioavailable ammonium (NH_4^+) [15]. In oligotrophic ocean regions, nitrogen fixation is important and can sustain more than half of the new production [16, 17]. Studies on nitrogen fixation in the AO are relatively few [18]. However, sequencing-based studies on the nitrogenase gene (*nifH* – a biomarker for diazotrophs [19]) have reported a wide distribution of putative diazotrophs in the AO with dominance of non-cyanobacterial diazotrophs (NCDs; e.g [20–23]). This is in contrast to lower latitude tropical and subtropical oceans where Cyanobacteria tend to be the dominant diazotrophs (e.g [24–26]). However, although not generally dominant, cyanobacterial diazotrophs are also present in some parts of the AO, including the Chukchi, Bering and Beaufort Seas [21, 27, 28] and the Fram Strait [29]. Furthermore, a few studies have reported nitrogen fixation rates from the Pacific sector of the AO (Chukchi, Bering, and Beaufort Sea [27, 28, 30]), Baffin Bay and the Canadian Arctic Archipelago with detectable rates ranging from 0.02 nmol N L^{-1} d^{-1} (Baffin Bay; [20]) to 17.2 nmol N L^{-1} d^{-1} (Chukchi Sea; [30]). This suggests that nitrogen fixation rates can at least occasionally be similar to rates measured in lower latitude regions. However, data are scarce, and although nitrogen fixation is widespread in the North Atlantic Ocean [31], it has not yet been reported from the Atlantic sector of the AO, hampering a pan-Arctic understanding of the potential importance and environmental regulation of nitrogen fixation.

The Fram Strait serves as a major gateway to the AO. On its western sector, it is characterized by the outflow of Polar water with the East Greenland Current (EGC) – which is an extension of the Transpolar Drift transporting shelf-influenced waters across the AO into the North Atlantic – and the inflow of Atlantic water (AW) with the West Spitsbergen Current (WSC) to the east (e.g [32]). The relatively fresh Polar water (temperature < 0 °C and salinity < 34.4) in the EGC accounts for about 30% of the total Arctic freshwater export [33], while the WSC transports warm, saline AW (temperature >3 °C; salinity >34.9) into the AO (e.g [34]). The distinct hydrography across the strait generates a frontal zone (FZ) that acts as a barrier, defined by marked gradients in e.g., sea-ice coverage [35], water chemistry [36–38], bio-optical properties [39], plankton communities [40–42] and overall carbon export [43, 44]. Thus, the Fram Strait offers a valuable opportunity to capture the characteristics of waters both exiting and entering the AO, reflecting both up- and downstream conditions.

Here, we aimed to elucidate the environmental drivers of nitrogen fixation and identify the key diazotrophic communities across the contrasting water regimes in the Fram Strait. Being a main gateway to the Arctic Ocean, information about diazotrophs and their activity is important for ultimately understanding and predicting nutrient biogeochemistry and productivity in the Arctic Ocean.

Materials and Methods

Study Regimes and Core Environmental Parameters

Samples were obtained onboard the R/V *Kronprins Haakon* during the FS2021 expedition from 31 st July to 20th August 2021. The sampling covered depths from 5 to 2620 m across three distinct hydrographic regimes in the Fram Strait; EGC, WSC, and their Frontal Zone (FZ) (Fig. 1). Temperature, salinity and chlorophyll-*a* (chl) fluorescence profiles were measured with a SBE911 CTD (Sea-Bird Scientific, WA, USA), and seawater samples were collected using Niskin bottles attached to the CTD-rosette system. To examine spring bloom dynamics daily chl concentrations were obtained from the Copernicus Marine Service product Arctic Ocean Biogeochemistry Analysis and Forecast (Product ID: ARCTIC_ANALYSISFORECAST_BGC_002_004). This Level-4 product is generated by the operational TOPAZ5-ECOSMO Arctic Ocean system, which couples the ECOSMO biogeochemical model to the TOPAZ5 physical model using the FABM framework. The product provides daily 3D fields of biogeochemical variables across the Arctic Ocean (50°–90°N, 180°W-180°E) at 6.25 km spatial resolution. Chl maps were produced for 2nd May, 2nd June, 2nd July, and 2nd August 2021. Concentrations of nitrite (NO_2^-), phosphate (PO_4^{3-}), and silicate ($Si(OH)_4$) were measured with a SmartChem 200 discrete nutrient analyser following Hansen and Koroleff [45]. Nitrate (NO_3^-) concentrations were measured using the vanadium chloride reduction technique [46]. Nutrient samples were stored at 4 °C and measured onboard within 24 h. Detection limits (NO_3^-; 0.1 µM, NO_2^-; 0.03 µM, PO_4^{3-}; 0.05 µM and $Si(OH)_4$; 0.5 µM) were determined by replicate measurements of reference seawater (KANSO, Technos Co., Ltd., Japan) every 10 samples. During the running of the samples from the cruise, over 40 determinations of each nutrient and each certified reference material (CRM) was performed. Three CRMs were used to follow the performance of the measurements: low (batch CK), medium (batch CL) and high (CO). Average accuracy (percent deviation from certified measurement) based on the CL/CO CRMs was 0.4/0.6, 0.05/0.01, 0.003/0.002, 0.008/0.007% for NO_2^-, PO_4^{3-}, $Si(OH)_4$ and NO_3^-, respectively. Average precision (coefficient of

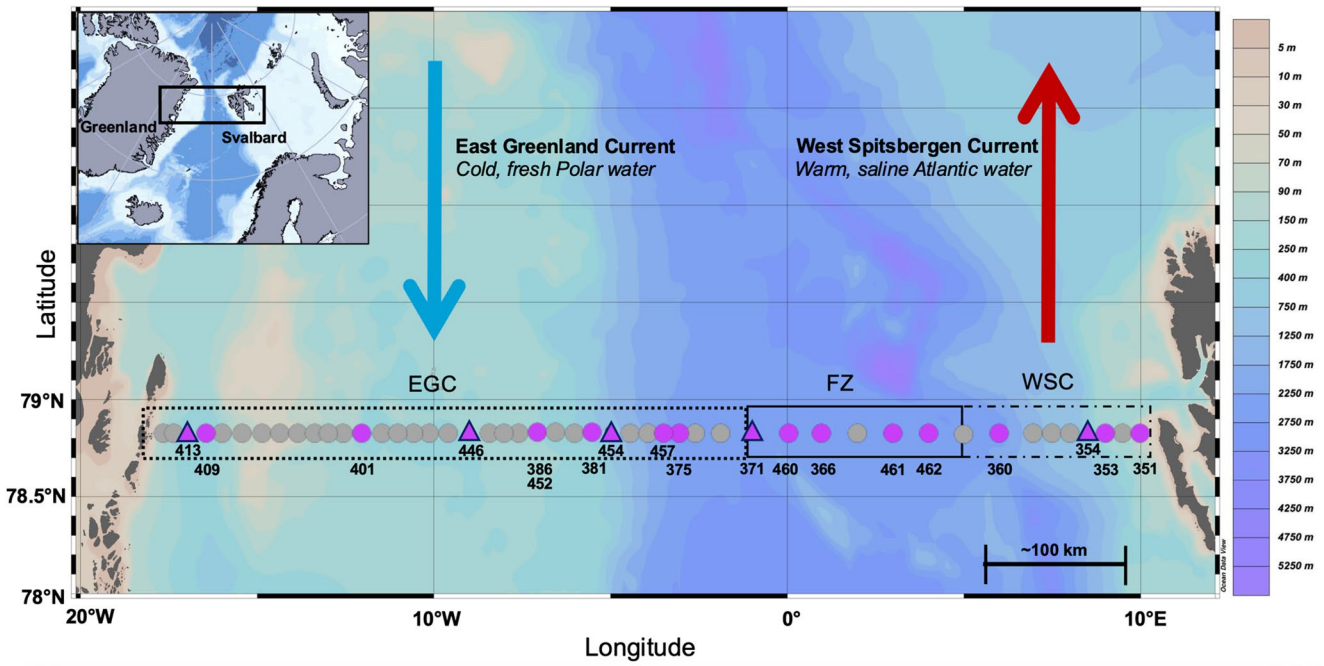

Fig. 1 Map of the study region with the FS2021 cruise track. Samples were collected from three divergent water regimes: WSC (West Spitsbergen Current), EGC (East Greenland Current) and their FZ (Frontal Zone). Nucleic acids were collected at all purple stations from four depths (5 m, 25–50 m, 100 m and 5–10 m above the seafloor). Purple triangles are stations where nitrogen fixation and primary production rates were measured from four depths. Numbers indicate station IDs, with stations 386 and 452 being sampled twice. Ancillary data was collected from all grey and purple stations. Produced with Ocean Data View and ggOceanMaps [48, 49]

variance) based on analyses on the same CRMs was 11/2.9, 3.7/2.8, 1.0/0.7, 2.0/0.9% for NO_2^-, PO_4^{3-}, $Si(OH)_4$ and NO_3^-, respectively. The Redfield N: P ratio [47] was calculated as $([NO_2^-] + [NO_3^-])/([PO_4^{3-}])$, leaving out ammonium, as these data were not available.

Samples for the analysis of coloured dissolved organic matter (CDOM) were filtered through 0.2 µm Millipore Opticap XL filter capsules into pre-combusted amber glass vials and kept in the dark at 4 °C until analysis onboard within 1–2 days. CDOM absorbance was measured across the spectral range from 250 to 700 nm using a Shimadzu UV–2401PC spectrophotometer and 100 mm quartz cells with ultrapure water as reference [50]. CDOM absorbance was then converted into an absorption coefficient (m^{-1}). In this study, we report the CDOM absorption coefficient at 254 nm (a254), hereafter referred to as CDOM.

Nitrogen Fixation and Primary Production Rate Measurements

As the sampling cruise was not dedicated to nitrogen fixation work, it was only logistically feasible to measure nitrogen fixation and primary production from four depths (5 to 2551 m) from five stations (Fig. 1; Table S1). Triplicate samples were transferred to acid-washed 4.6 L polycarbonate bottles. In addition, one reference bottle (2.5 L, time zero, T_0) was immediately filtered onto glass fiber filters (Advantec™ GF75, pre-combusted at 450 °C for 6 h, 25 mm, nominal pore size 0.3 µm, Toyo Roshi Kaisha, Ltd., Japan) at 4 °C to obtain in situ $^{15}N/^{14}N$ and $^{13}C/^{12}C$ isotope ratios and particulate organic nitrogen (PON) and carbon (POC) concentrations. Nitrogen fixation rates were measured following the bubble release method [51] where all bottles were closed bubble-free with septa screw caps and spiked with 6 mL high purity $^{15}N_2$ gas (99%, Cambridge Isotope Labs, MA, USA). To enhance $^{15}N_2$ dissolution, all bottles were gently shaken continuously for 15 min at 2–5 °C until the removal of remaining gas [51]. Primary production rates were measured by parallel addition of $NaH^{13}CO_3$ (93 µM, ≥ 98 atom%, Sigma Aldrich, MA, USA) targeting an enrichment of ~ 5% of the expected in situ dissolved inorganic carbon concentration in the Fram Strait [52].

Samples were incubated for 24 h in a transparent on-deck container with flow-through surface seawater, maintaining temperature within ± 1.5 °C of in situ conditions. Bottles were shaded with black nylon mesh or plastic so that light exposure mimicked in situ photosynthetic active radiation, with meso- and bathypelagic samples incubated in the dark.

Post incubation, duplicate 12 mL gas-tight exetainers (Labco, Lampeter, UK) were filled from each bottle and stored upside down, submerged in seawater in darkness at 4 °C for the analysis of $^{15}N_2$ atom% by membrane inlet mass spectrometry [53] within three months. The remaining

sample water was filtered onto pre-combusted Advantec filters and stored at −20 °C until dried onboard (50 °C, 24 h). POC and PON concentrations were analysed using a coupled Elemental-Analyzer to Isotope-Ratio-Mass Spectrometer (IRMS; Integra 2, SerCon Ltd) as described in Benavides et al. [54]. Limit of quantification (LOQ) for PON was 2 µg N per sample with linearity throughout all measurements (2–500 µg N). The range of $^{15}N_2$ enrichments was − 20.8–54.6‰ (median 5.2‰). Nitrogen fixation rates were calculated according to Montoya et al. [55], following White et al. [56] with error-propagation-based limit of detection (LOD) calculations [57] (Supplementary Datasheet S1). Primary production rates were calculated according to Hama et al. [58] (Supplementary Datasheet S2). The contribution of measured nitrogen fixation to the nitrogen demand for in situ net primary production was estimated using the Redfield ratio [47]. To account for potential differences in elemental stoichiometry [59] across the Fram Strait, the in situ molar C: N ratios were used for this calculation in parallel (Table S1). The calculation of the potential contribution of nitrogen fixation to primary production is based on the amount of new nitrogen added to the system and theoretically becoming available for primary producers through leakage and eventual remineralisation of diazotroph cells. Uncertainty in the calculated contribution was estimated from the standard deviations of triplicate measurements of nitrogen fixation and primary production, applying standard error propagation to account for variability in both rates.

Diazotroph Community Analysis

DNA was obtained from 5 m, 25–50 m, 100 m, and just above the bottom at 19 stations (Fig. 1). Seawater was immediately filtered onto 0.22 µm Sterivex filters (Millipore, MA, USA) at 4 °C (2–4 L; maximum duration 45 min) and stored at −80 °C. Prior to DNA extractions, filters were removed by cutting open one end of the plastic casing. Filters were thoroughly grinded with a sterile metal pestle whilst being flash frozen (up to 8 times) with liquid nitrogen in between grinding. DNA was extracted using the AllPrep DNA/RNA Mini Kit (Qiagen Sciences, MD, USA), stored at −20 °C, and quantified using PicoGreen (Quant-iT, Invitrogen, MA, USA). *nifH* gene amplicons were generated in 25 µL nested polymerase chain reactions (PCRs) [60] using PuReTaq Ready-To-Go™ PCR beads (Cytiva, Marlborough, MA, USA). Primers nifH3 and nifH4 [61] were used for the outer PCR reaction (0.4 µM), and $MgCl_2$ was added (5 mM). For inner PCR reactions, primers nifH1 and nifH2 [62] were used (0.4 µM), and $MgCl_2$ (2.5 mM) was added. DNA template (median 7.2 ng) was added to the outer PCR reaction, followed by transferring 1 µL of the produced product to the inner PCR reaction. Samples were amplified in triplicate for 30 cycles at 94 °C (60 s), 54 °C (60 s), and 72 °C (60 s) with a first and final step at 94 °C (120 s) and 72 °C (420 s), respectively. Size and purity were checked for all samples by agarose gel electrophoresis. Triplicate inner PCR products were pooled, purified (GeneClean Turbo, MP Biomedicals, CA, USA), and quantified (PicoGreen). In 26 of 76 samples, unspecific amplification was seen and therefore, *nifH* bands were gel-extracted and purified (PureLink™ Quick Gel Extraction Kit, Invitrogen) from these. Negative controls containing UV-irradiated PCR-grade water as template were included in all PCR rounds, and one pooled triplicate set was included for sequencing. Five ng of all pooled amplicons and gel-extracted bands were indexed in 25 µL reactions using Illumina indexes (National Genomics Infrastructure, Uppsala, Sweden), 0.25 µL MyTaq™ Red DNA polymerase (Bioline, Meridian Bioscience, UK), 0.4 µM barcoded forward and reverse primers, 3.5 mM $MgCl_2$, and 8 cycles at 94 °C (30 s), 62 °C (30 s), 72 °C (30 s) starting and ending with 94 °C (60 s) and 72 °C (300 s), respectively.

Indexed pooled amplicons were purified (Agencourt, Beckman Coulter, CA, USA), quantified (PicoGreen), pooled in equimolar ratios, and sequenced at the Geo Genetics Sequencing Core, University of Copenhagen, Denmark using an Illumina MiSeq v3 (paired-end, 2 × 300 bp) platform.

Sequence Analyses

Sequence analyses were done as follows: (1) Generation of amplicon sequence variants (ASVs) with the DADA2-pipeline (v. 1.26.0; [63]) with read-trimming at 240 (forward) and 170 (reverse), (2) Removal of non-*nifH* reads and *nifH* homologs using steps 2, 4 and 5 of the NifMAP pipeline (v.1.0; [64]; 680 ASVs removed), (3) Assigning of *nifH* phylogenetic clusters [65], (4) Assigning of *nifH* taxonomy (assignTaxonomoy; DADA2) based on a *nifH* database [66, 67]. ASV contaminants were identified using decontam (v.1.12.0; [68]). All data analyses were performed in R-4.1.1 [69] using phyloseq (v.1.36.0; [70]) and vegan (v.2.6.4; [71]). Samples with < 200 reads (13 of 76 samples) were removed. The ASVs with no assigned taxonomy from the DADA2 pipeline were grouped as "NA". The nearest relatives of the 20 most abundant ASVs (accounting for 62% of all reads) and the 10 ASVs representing >25% of the relative abundance in samples where nitrogen fixation was measurable were additionally identified (nucleotide similarity) using the NCBI database (https://blast.ncbi.nlm.nih.gov/). These ASVs, their nearest relatives, and selected

Arctic reference sequences were aligned with MAFFT (L-INS-I [72]), and used to build a maximum likelihood tree in raxmlGUI (v. 2.0.13; [73]) with 1000 bootstraps. The ModelTest-ng (raxmlGUI) was applied to find the optimal substitution model and rate heterogeneity settings for the tree (G4, gamma mean). Visualization of the tree was done using iTOL [74].

Quantification of Dominant Arctic Betaproteobacteria

A dominant group of ASVs (ASV1, 10, 34, and 42) belonged to a Betaproteobacteria group named Beta-Arctic1 and was quantified in 21 samples (where *nifH* gene amplicon reads for this group was >100) with quantitative PCR (qPCR) using the assay developed in von Friesen et al. [75]. In brief, triplicate 13 µL reactions containing 1 x LightCycler® 480 Probes Master mix (Roche, Basel, Switzerland), 0.5 µM primers, 0.2 µM probe, and 2.5 ng DNA were run. A serial dilution of standard (gBlocks) was used (10^0–10^9 gene copies), and the qPCR efficiency was 99.57%. A negative control (PCR grade water) and duplicate inhibition controls (environmental DNA sample tested against a standard concentration of 10^6 gene copies) generated no amplification and no inhibition, respectively. The limit of detection (LOD) and limit of quantification (LOQ) were calculated for each sample based on blank and low-concentration sample variability [76].

Statistical Analyses

Alpha-diversity was assessed using median-normalized sequence data containing singletons, but singletons were removed for other statistical testing. To evaluate differences in alpha-diversity across the three hydrographic regimes (EGC, FZ, and WSC), the Shannon diversity index was calculated using the estimate_richness() function from the phyloseq package [70]. To test if community composition differed between regimes and depth categories, a PERMANOVA was conducted on centered log ratio transformed data (clr; transformed with the compositions package; [77]) using the adonis2() function from the vegan package [71] based on Euclidean distance with 999 permutations. Additionally, pairwise.adonis [78] was used to identify differences between regimes. In parallel, the function betadisper was used to ensure homogeneity of group dispersions. The envfit function (vegan package v.2.6.4; [71]) was used to investigate relationships between selected ancillary data (temperature, salinity, NO_2^-+NO_3^-, $Si(OH)_4$, PO_4^{3-}, and CDOM) and principal components on clr transformed data. The envfit analysis was performed using 999 permutations, and p-values were adjusted using the Bonferroni correction to account for multiple testing. Redundancy analysis (RDA) was used to ordinate and evaluate if any ancillary data were significant drivers of community composition. Principal component analysis (PCA) was performed using the prcomp() function to evaluate the three hydrographic regimes based on ancillary data. To assess differences in ancillary data among the three regimes, one-way ANOVA was applied when assumptions of normality (verified using the Shapiro-Wilk test) and homogeneity of variances (validated with Levene's test) were met, followed by Tukey's HSD post hoc test. The non-parametric Kruskal-Wallis test was applied when data did not meet the criteria for a one-way ANOVA. In cases where the Kruskal-Wallis test revealed significant differences, Dunn's post hoc test with Bonferroni correction was applied to identify pairwise differences between regimes. Spearman's Rank correlation was used to find correlations between ancillary data and nitrogen fixation rates above LOD, primary production, and *nifH* gene copies of Beta-Arctic1, respectively. For all statistics, analyses with p-values < 0.05 were considered significant. Data visualization was done using ggplot2 [79], ggOceanMaps [49], microViz [80], microshades [81], and Ocean Data View [48].

Results

Environmental Gradients Across Fram Strait

Pronounced environmental gradients were observed between the Polar waters in the East Greenland Current (EGC) and Atlantic waters in the West Spitsbergen Current (WSC), with intermediate values in the Frontal Zone (FZ) (Fig. 2; Fig. S1; Table S2). The differences between hydrographic regimes were statistically confirmed (Table S2). Temperature and salinity were higher in WSC compared to EGC ranging from − 1.8 °C (EGC) to 6.7 °C (WSC) and 22.5 (EGC) to 35.0 (WSC), respectively (Fig. 2). Across all sample depths, concentrations of NO_2^-+NO_3^- were also higher in WSC (average 7.1 ± 5 µM) compared to EGC (5.3 ± 4.8 µM). The same trend was observed in the upper 100 m where concentrations of NO_2^-+NO_3^- averaged 4.2 ± 3.8 µM and 2.3 ± 2.8 µM in WSC and EGC, respectively. Additionally, chl fluorescence (Fig. 3) in the upper 100 m was also higher in WSC (average 1.8 ± 1.4) compared to EGC (average 0.3 ± 0.5). Chl concentration maps for 2nd May, 2nd June, 2nd July, and 2nd August 2021 showed that the spring bloom was over when sampling occurred (Fig. S2). CDOM and $Si(O)_4$ were higher in the EGC compared to the WSC, while PO_4^{3-} did not differ among the three regimes (Fig. 2). Based on the Redfield ratio, nitrogen was limited relative

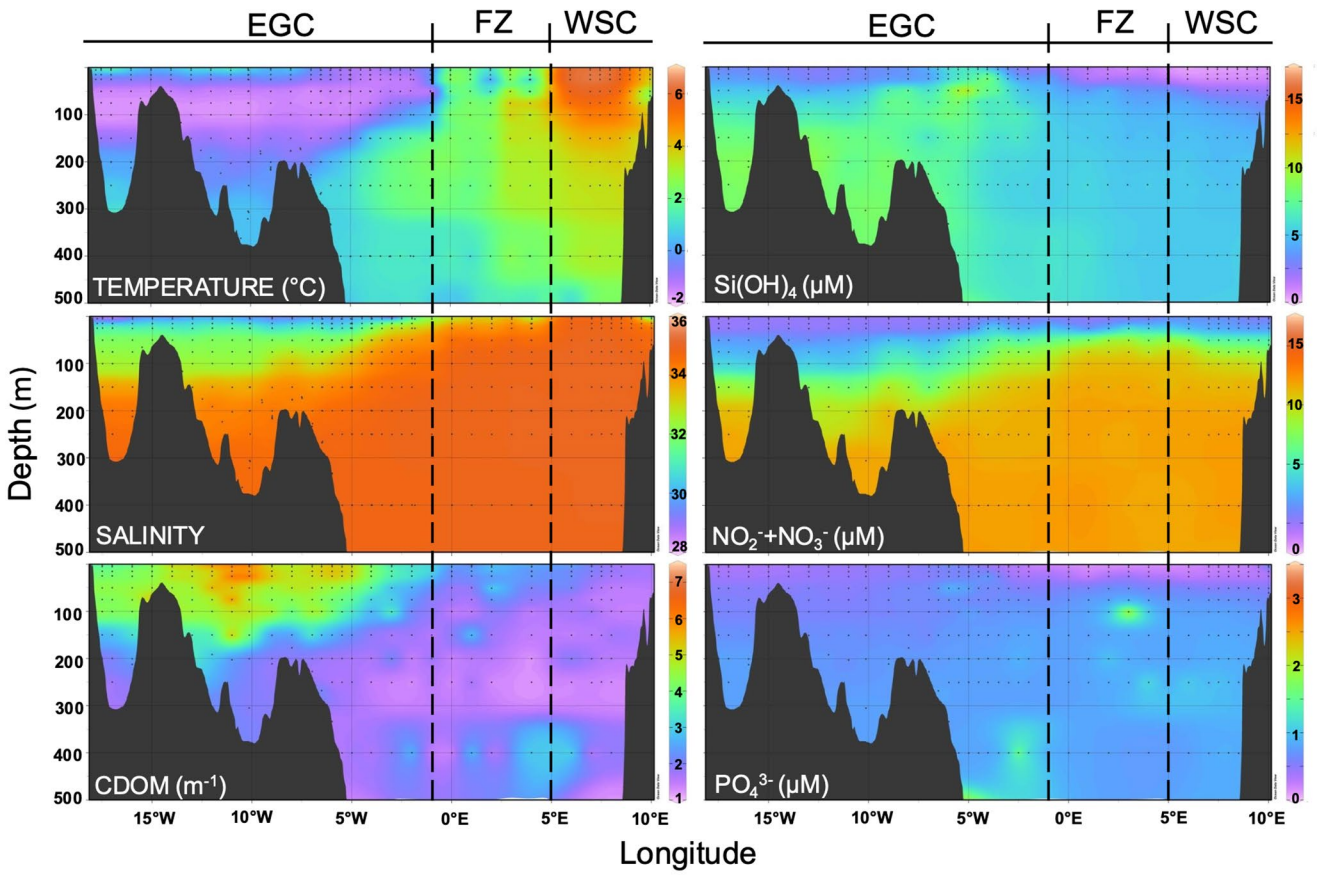

Fig. 2 Environmental conditions across the Fram Strait (0–500 m) covering the three regimes: WSC (West Spitsbergen Current), EGC (East Greenland Current) and their FZ (Frontal Zone). CDOM refers to coloured dissolved organic matter absorption coefficient measured at wavelength 254 nm (m^{-1}). For chlorophyll fluorescence profiles, see Fig. 3. Produced with Ocean Data View [48]

to phosphorus (N: $P<16$) at all locations and depths where DNA was sampled (including stations where nitrogen fixation and primary production were measured), except for two deep samples (Table S1).

Nitrogen Fixation and Primary Production

Nitrogen fixation was measured at four depths of five stations. Rates were above LOD in 9 of the 20 water samples, including at 5 m at all stations, but always below LOD at depths greater than 100 m (Fig. 3, Table S1; Supplementary Datasheet 1). In general, rates above LOD were low and ranged from 0.02 ± 0.01–0.73 ± 0.7 nmol N L^{-1} d^{-1} across EGC and PF, however, elevated nitrogen fixation rates were found at the one station in WSC, ranging from 0.32 ± 0.1–10.15 ± 4.9 nmol N L^{-1} d^{-1} (Fig. 3).

Spearman's Rank correlation analysis revealed positive correlations between nitrogen fixation rates and temperature ($p<0.05$, rho = 0.47, $n=9$; Fig. S3), and chl fluorescence ($p<0.05$, rho = 0.73, $n=9$; Fig. S3). Negative correlations were identified between nitrogen fixation rates and CDOM ($p<0.05$, rho = −0.78, $n=9$; Fig. S3), and $Si(OH)_4$ ($p<0.05$, rho = −0.82, $n=9$; Fig. S3).

Primary production rates (Table S1; Supplementary Datasheet 2) varied between EGC and WSC (one-way ANOVA; $p<0.05$, $F=4.2$), spanning from 3.81 ± 0.21 (station 446; 5 m, EGC) to 9,573 ± 3,527 nmol C L^{-1} d^{-1} (station 354; 5 m, WSC). It was positively correlated with nitrogen fixation (Spearman's Rank, $p<0.001$, rho = 0.93, $n=9$; Fig. S3) and chl fluorescence (Spearman's Rank, $p<0.001$, rho = 0.82, $n=20$). The nitrogen fixation could theoretically account for 0.3% ± 0.3% (station 371; 5 m; FZ) to 16.9% ± 12.3% (station 446; 5 m; EGC) of the nitrogen required for the measured primary production (based on the Redfield/in situ C: N molar ratio), with the largest contribution in samples where primary production rates were low (Table S1).

Composition and Distribution of Diazotrophs

The *nifH* gene amplicon library included 792 ASVs. At the class level, NCDs, ASVs of unknown taxonomy, and Cyanobacteria accounted for 77.3%, 18.9%, and 3.8% of all reads, respectively (Fig. 4). *nifH* gene clusters showed similar

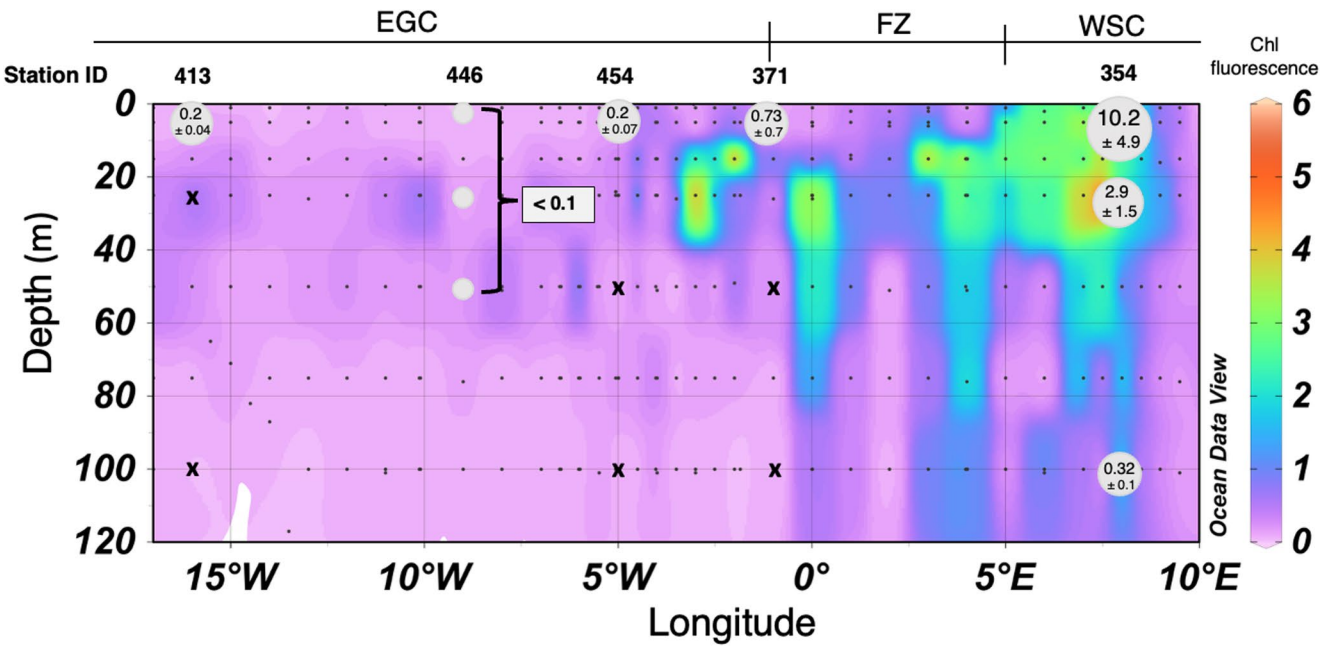

Fig. 3 Average nitrogen fixation rates (nmol N L^{-1} d^{-1}) shown in circles (not to scale) from triplicate samples with one standard deviation across the surface layer of the Fram Strait (0–120 m). WSC; West Spitsbergen Current), EGC; East Greenland Current and FZ; Frontal Zone. Black crosses indicate samples where nitrogen fixation was below the limit of detection. Chlorophyll (Chl) fluorescence is shown as background due to the correlation with nitrogen fixation rates above LOD (Spearman's Rank; $p = 0.03$, rho = 0.73). Produced with Ocean Data View [48]

representation in the three regimes, with Clusters I and III accounting for 62% and 27% of all reads, respectively (Fig. S3). Beta-, Delta-, and Gammaproteobacteria accounted for >50% of the relative abundance in 37 of the 63 samples, whereas Cyanobacteria dominated in three samples (all from 25 m; Fig. 4). Despite the large variability among samples, diazotroph community composition (pairwise adonis, $p>0.05$) and alpha diversity (Shannon index, one-way ANOVA, $p>0.05$) did not differ significantly among the three regimes of the Fram Strait (all samples merged for each regime). Community composition was, however, different between 5 m and >100 m (adonis2, $p<0.01$, $R^2=0.07$), 25 m and >100 m (adonis2, $p<0.01$, $R^2=0.06$), and 100 m and >100 m (adonis2, $p<0.05$, $R^2=0.06$). The envfit analysis showed no significant environmental drivers (temperature, salinity, NO_2^-+NO_3^-, $Si(OH)_4$, PO_4^{3-}, and CDOM) of community composition (for all, $p>0.05$; data not shown).

A deeper phylogenetic analysis was conducted of the 20 ASVs with the highest relative abundance and the 10 main ASVs (four of these were among the overall top 20 ASVs) found in the samples where nitrogen fixation was measurable (Table S3, Fig. 5). The 20 dominant ASVs each represented 1.2 to 11.4% of the total reads and collectively accounted for 62% of all reads. Eight ASVs were classified as 'unknown' and only two of these (ASV 8 and 20) exhibited high similarity (>99%) to previously found environmental sequences (Table S3). Six ASVs exhibited high similarities (93.6–100%) to bacteria previously found in the AO, and nine ASVs showed low similarities (< 92%) to their nearest relatives (Table S3). The dominant ASVs from samples where nitrogen fixation was detectable (Fig. 5; shown in green) differed among the three regimes (WSC: ASVs 2, 71, 105, 114; FZ: 5, 46; EGC: 11, 13, 33, 48), and only ASVs 5 and 13 exhibited high similarity (>99%) to sequences previously found in the Central AO [82]. Five of the ASVs showed similarities of 93.6–97.7% to their nearest relatives in the database, and the remaining three showed only low similarity (< 90%) to any known environmental sequences (Table S3). A Gammaproteobacterium (ASV 105) dominated (relative abundance 90%) in the sample where the highest nitrogen fixation rate was measured (WSC; station 354; 5 m). Overall, the dominant ASVs belonged to Clusters I, III, and IV and were phylogenetically diverse, with six of 20 ASVs previously found in the AO (Fig. 5).

The most abundant ASV (ASV 1) accounted for 11.4% of all reads (Table S3). It was identical to a sequence found in WSC and belonged to the Beta-Arctic1 group, earlier reported from several locations of the AO and recently found to be expressing *nifH* in the Atlantic gateway to the AO [75]. ASVs 10, 34, and 42 were also affiliated with this group. Quantification of the Beta-Arctic1 group by qPCR was above the limit of detection in 7 of 21 samples with

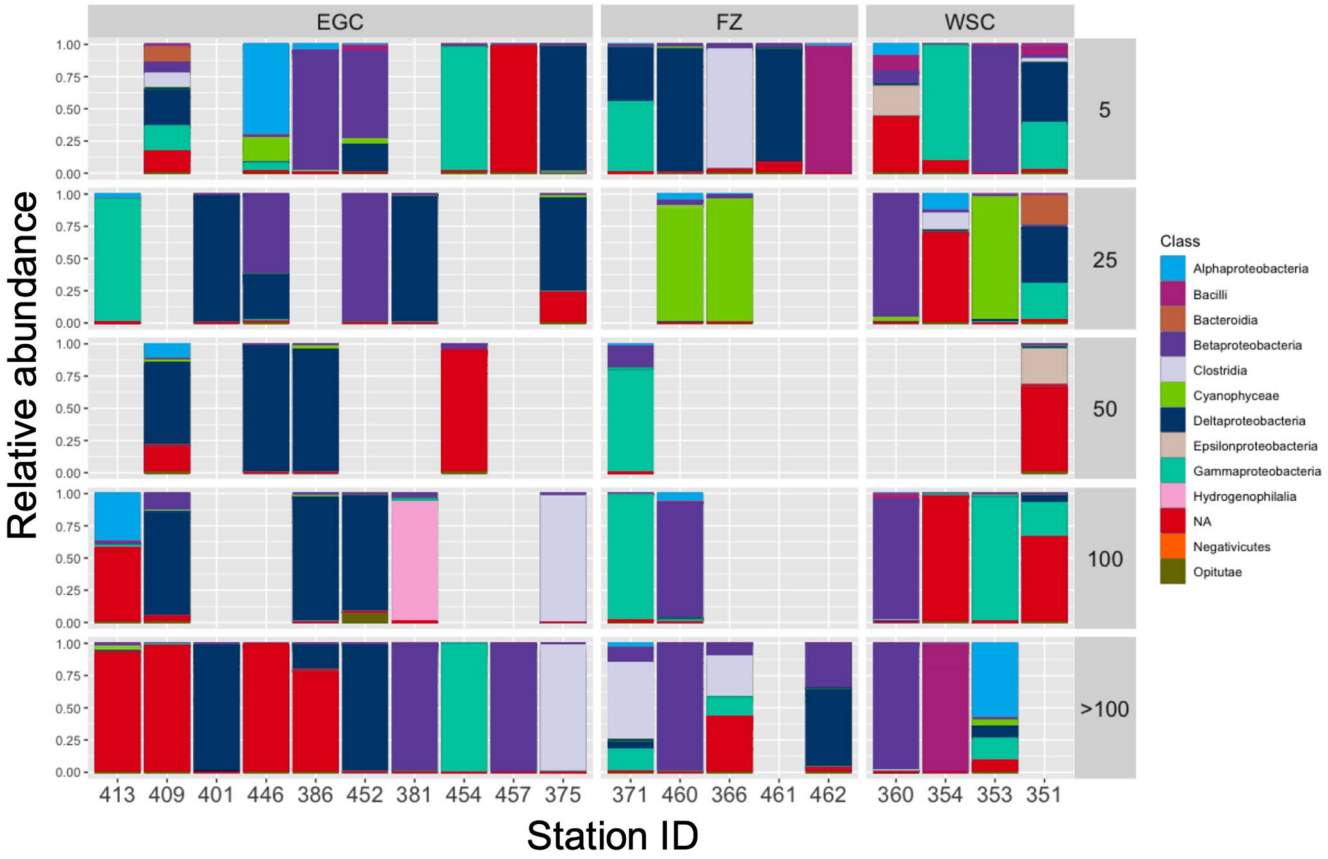

Fig. 4 Diazotroph community composition across the Fram Strait and the three regimes WSC (West Spitsbergen Current), EGC (East Greenland Current), and their FZ (Frontal Zone). Relative abundance of classes of diazotrophs based on *nifH* amplicon sequencing sorted by depth. Blank spaces indicate samples discarded after the sequence quality control or depths not sampled. Samples assigned "NA" are classes with unknown taxonomy (see 'Sequence analyses')

nifH gene abundances ranging from 664 to 6,741 copies L^{-1} (Fig. 6). It was reported from the surface to 100 m depth, and only quantifiable in WSC and FZ, with the highest gene copies L^{-1} in WSC (Kruskal-Wallis, $p < 0.05$). Spearman's Rank Correlation analysis revealed positive correlations of Beta-Arctic1 *nifH* gene copies L^{-1} to temperature ($p < 0.001$, rho = 0.67, $n = 21$), salinity ($p < 0.05$, rho = 0.44, $n = 21$), and chl fluorescence ($p < 0.001$, rho = 0.51, $n = 21$).

Furthermore, a negative correlation was found to $Si(OH)_4$ ($p < 0.01$, rho=−0.55, $n = 21$).

Discussion

Nitrogen Fixation and its Potential Importance as a Nitrogen Source

Nitrogen fixation was measurable across the Fram Strait and differed significantly between the regimes, with lowest rates found in the EGC ranging between 0 and 0.2 nmol N L^{-1} d^{-1} in surface waters (Fig. 3). These low rates are comparable to those reported from other Arctic regions, such as the Chukchi Sea (0.17 ± 0.19 nmol N L^{-1} d^{-1}; [28]), Baffin Bay, and the Canadian Arctic Archipelago (0.08 ± 0.06 and 0.02 ± 0.46 nmol N L^{-1} d^{-1}, respectively; [20]). Hence, low nitrogen fixation rates appear common in diverse and geographically widespread regions of the AO, including the EGC of the Fram Strait. In contrast, two of the four nitrogen fixation rates measured in the WSC were up to two orders of magnitude higher, ranging from < LOD (568 m) to 10.15 nmol N L^{-1} d^{-1} (5 m) (Fig. 3). These are, to our knowledge, the first reported rates from this region, and comparable with rates measured during the same time of year (July – September) in coastal waters of the Chukchi Sea averaging 7.7 ± 1.8 nmol N L^{-1} d^{-1} [30] and in the Bering Sea (6.9 nmol N L^{-1} d^{-1}; [28]). Other studies from the Bering and Chukchi Seas only reported rates up to ~ 3 nmol N L^{-1} d^{-1}, although these rates were measured in a different season (September/October; [21, 27]). Together, these few results may suggest an influence by season, with higher nitrogen fixation rates in summer and lower rates in fall in the AO. Indeed, diazotrophic community composition varies with season in this region [22], however, whether nitrogen fixation rates vary

Fig. 5 Maximum-likelihood phylogenetic tree (partial *nifH* amino acid sequences) for the 20 most abundant amplicon sequence variants (AVSs) and ASVs dominant at the stations where nitrogen fixation was measurable (shown in green; see Table S3). Reference sequences are nearest relatives from the NCBI database. Arctic reference sequences are displayed in blue. Clusters are *nifH* phylogenetic clusters [83]. Cluster I includes Cyanobacteria, Firmicutes, Beta- and Gammaproteobacteria whereas Cluster III includes Deltaproteobacteria

with season in Fram Strait is unknown since we only sampled during summer. Nevertheless, this is likely because the region is exposed to large seasonal differences in hydrography and biochemistry [84].

Interestingly, nitrogen fixation was mainly detected at 5 m and occasionally at 25 m (WSC, EGC), 50 m (EGC) and 100 m (WSC), suggesting an overall direct or indirect link to light-driven processes. This could potentially be explained by light reaching deeper in WSC compared to EGC due to the lack of sea ice and/or the lower CDOM concentrations in the WSC [39]. Comparative data from deeper waters in the AO are scarce, but one study from ~ 90 m depth from water off the Chukchi Sea shelf reported similar low rates (0–0.57 nmol N L^{-1} d^{-1}; [21]). As no light data was available to us, potential links between nitrogen fixation and light could not be explored further. We encourage future studies to explore

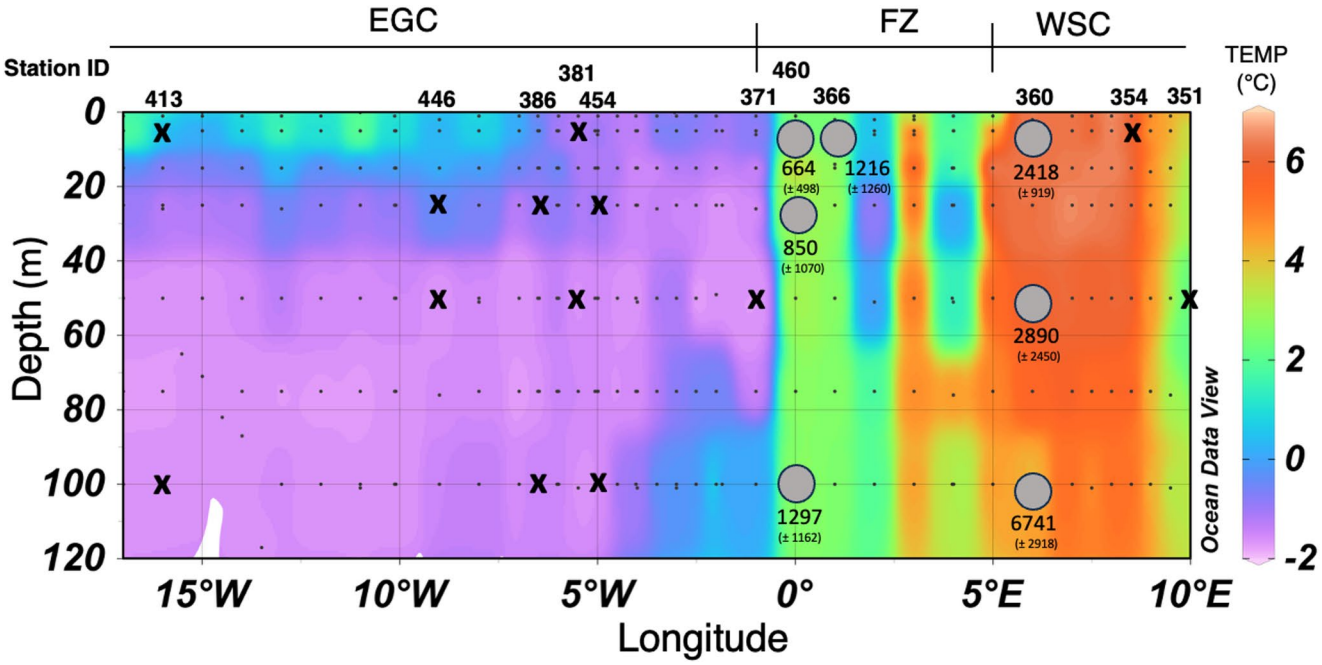

Fig. 6 Distribution of the Beta-Arctic1 group across the Fram Strait (0–100 m) based on quantitative PCR. EGC (East Greenland Current), FZ (Frontal Zone) and WSC (West Spitsbergen Current) refers to the three water regimes. Circles represent samples where the *nifH* gene abundance was higher than the limit of detection. Numbers are in average *nifH* gene copies L^{-1} ± one standard deviation. Black crosses indicate samples where the Beta-Arctic1 group was not quantifiable. Samples are displayed with temperature (°C) as background due to the correlation found between *nifH* gene copies L^{-1} and this parameter (Spearman's Rank; $p < 0.001$, rho = 0.67). Produced with Ocean Data View [48]

this and evaluate the importance of nitrogen fixation below the euphotic zone in the AO.

We speculate that the nitrogen fixation rates measured in this study were mostly attributed to heterotrophic diazotrophs, as previously observed in some regions of the AO [20–22, 75]. This activity could be driven partly by bioavailability of DOM freshly produced by the contemporary phytoplankton biomass, ultimately linked to a supply of inorganic nitrogen (DIN). The concentration of NO_2^-+NO_3^- in surface waters of the WSC was higher than in the EGC in our dataset (Table S1), as previously seen [85], conceivably supporting higher primary production. For instance, at station 354 in the WSC, chl fluorescence and primary production rates were elevated relative to other stations (Fig. 3; Table S1). The expected release of DOM from this phytoplankton biomass [37, 86] could stimulate nitrogen fixation activity by NCDs; however, it is also likely that the high nitrogen fixation in the WSC was stimulated by the high temperature (see also below). Indeed, at station 354 we measured the highest nitrogen fixation rates, however, this higher absolute N input from nitrogen fixation, did not mirror the potential contribution to in situ primary production (0.6–5.3%). Hence, although the release of bioavailable N via nitrogen fixation is relatively higher in the WSC, it may not be important to co-occurring phytoplankton. On the other hand, the lower nitrogen fixation rates in EGC could support up to 16.9 ± 12.3% of new in situ primary production, possibly explained by the low DIN concentration. This potential of relatively high support is similar to findings from the Pacific sector of the AO (Chukchi Sea), where nitrogen fixation may support up to 17% of new primary production [21]. However, it should be noted that most of our nitrogen fixation rates are close to the LOD, and the calculated support of new primary production should therefore be treated with caution. Moreover, the support could be overestimated given that some diazotrophs, cyanobacteria and NCDs, may take up organic N sources [87].

Environmental Drivers of Nitrogen Fixation Across the Fram Strait

The measured nitrogen fixation rates were positively correlated with temperature, with lower rates in the cold EGC and higher rates in the warmer WSC. This is consistent with the general view of temperature as a regulating factor for nitrogen fixation in tropical and subtropical waters [88–90]. Sipler et al. [30] measured nitrogen fixation rates in the AO ranging from 3.5 to 17.2 nmol N L^{-1} d^{-1} at temperatures of 4.5–6.7 °C, and our data suggest that nitrogen fixation does decrease or is not detectable when entering the Polar waters of EGC with colder conditions (−2-2 °C). Interestingly,

such responsiveness to temperature was recently modelled for NCDs attached to particulate organic matter [91].

We found a negative correlation between nitrogen fixation and $Si(OH)_4$ concentrations and CDOM, with particularly low $Si(OH)_4$ concentrations in the WSC – the station with the highest nitrogen fixation, primary production rates and chl fluorescence. Moreover, nitrogen fixation was overall positively correlated with primary production, which has also been observed in the Central AO [92]. Indeed, primary production rates were more than two orders of magnitude higher in the WSC compared to the EGC, likely due to elevated concentrations of NO_2^-+NO_3^- in the Atlantic water stimulating phytoplankton growth [41, 85, 93]. We speculate that extensive phytoplankton growth in the WSC [94] prior to or during our sampling caused elevated levels of low-molecular weight, freshly produced DOM [37]. This idea is supported by elevated phytoplankton biomass earlier in the year (Fig. S2) and previous observations in the Fram Strait (WSC), where semi-labile DOM components were found to be higher in summer compared to autumn and correlated with phytoplankton biomass [95]. The study further reported a decline in bacterial production as semi-labile DOM components decreased, suggesting that DOM availability affects bacterial production. Additionally, freshly produced labile DOM associated with primary production can stimulate diazotrophy [54, 96] and DOM uptake or stimulation of nitrogen fixation has been shown for Cyanobacteria [97, 98] and NCDs [87, 99] in other marine regions. This idea has also been tested in the Central AO where nitrogen fixation was stimulated by an addition of labile dissolved organic carbon [92]. In our study, the highest nitrogen fixation was likely driven by NCDs as they dominated the WSC communities (see below). On the other hand, the negative correlation of nitrogen fixation to CDOM, is likely due to CDOM in the EGC being high and mainly of terrestrial origin [37, 100], which is less accessible as a carbon source for diazotrophs. Consequently, we suggest that the high nitrogen fixation in the WSC is driven by temperature, but also likely by availability of labile DOM of phytoplankton origin, despite the co-occurrence of inorganic nitrogen (Table S1). This is consistent with the earlier observations that pelagic nitrogen fixation occurs widely in waters replete in inorganic nitrogen [101].

Non-Cyanobacteria are the Dominant Putative Diazotrophs in the Fram Strait

The observed dominance of NCDs among the *nifH* gene reads and the parallel nitrogen fixation rates strengthen the view that NCDs are important players in Arctic nitrogen fixation [20–22, 75, 82]. Our samples were dominated by Proteobacteria (71% of all reads) mainly accounted for by Beta-, Delta-, and Gammaproteobacteria (53% of total reads; Fig. 4). Our most abundant ASV (ASV1; 11.4% of all reads) belonged to the so-called Beta-Arctic1 group, which has earlier been found actively expressing *nifH* in the WSC [75]. We recovered *nifH* genes of this group in all three regimes (Fig. 6). However, it was only quantifiable by qPCR in WSC and FZ with abundances ranging from 664 up to 6,741 *nifH* gene copies L^{-1} (Fig. 6). ASV1 showed 98.2% similarity to *Dechloromonas aromatica* found in soil and freshwater environments and thought to be associated with a eukaryotic host [102]. A strong correlation was found between ASV1 abundance (*nifH* gene copies L^{-1}) and temperature (Spearman's Rank; $p < 0.001$, rho = 0.67; Fig. 6) suggesting that temperature is important for the prevalence of this group. Interestingly, we also observed a positive correlation between Beta-Arctic 1 *nifH* gene copies L^{-1} and chl fluorescence, which could indicate an association with phytoplankton biomass. This is also in agreement with the negative correlation found to $Si(OH)_4$ ($p < 0.01$, rho=−0.55), suggesting a potential association with diatoms. Hence, we speculate that the peak abundance of Beta-Arctic1 *nifH* gene copies at 100 m depth (Fig. 6) was due to affiliation with sinking diatom particles (*sensu* particle-associated nitrogen fixation by NCDs [91]). Unfortunately, phytoplankton was not characterized in our study and the linkage to diatoms can therefore not be substantiated. We note that an association to diatoms was recently shown for an important NCD in the North Atlantic Ocean [103], and encourage future studies to examine such putative coupling of diazotrophs to diatoms also in the AO.

Surprisingly, despite being widely distributed (Fig. 6), ASV1 was not quantifiable at the locality with highest nitrogen fixation (station 354; WSC). In contrast, the gammaproteobacterial ASV105 accounted for 90% of the relative *nifH* gene abundance at this station. ASV105 displayed 97.7% similarity to a soil phylotype (Table S3), and belongs in subcluster 1G, which is widely found in the Eurasian Basin and Atlantic waters [75, 82]. While the high prevalence may indicate a key role of this phylotype, a causal relationship with the co-occurring high nitrogen fixation rates and identification of the importance of this putative Gammaproteobacterium would need to integrate *nifH* gene expression data. In general, Gammaproteobacteria are important diazotrophs in the oceans, with specific phylotypes like GammaA and Pseudomonas being widely distributed (reviewed in [104]). Indeed, Gammaproteobacteria were also prominent in our dataset, accounting for 10.5% of the overall *nifH* gene reads, but our dominant ASVs were only distantly related (< 85% similarity) to GammaA or to the Gamma-Arctic1 and Gamma-Arctic2 groups (Fig. 5, Table S3), which have earlier been found in the AO [75, 82]. However, ASV5 was 99.4% similar to a phylotype found in the Eurasian Basin of

the Central AO [82]. Moreover, some gammaproteobacterial ASVs occurred sporadically in discrete samples (e.g., stations 351, 353, 371, and 381; Fig. 4). Hence, our dataset offers only limited insight into the ecology of the gammaproteobacterial diazotrophs.

Overall, the dominant diazotrophs in the Fram Strait were mainly distantly related to known taxa, and only 6 out of the 20 dominant ASVs were identical or highly similar to *nifH* phylotypes previously reported from Arctic waters (Fig. 5, Table S3). This was also the case if only the dominant ASVs in samples where nitrogen fixation was measurable were taken into account (Table S3). Despite the limited sampling coverage of the AO to date [18], the low similarity of our *nifH* phylotypes to known taxa globally, and the match of only a few ASVs to taxa found earlier in the AO, suggest that Arctic diazotrophs are diverse and that some phylotypes are endemic [75, 82, 105, 106]. Interestingly, some Arctic-endemic diazotrophs have unique gene sets [106], hence, future research on the ecological and biogeochemical consequences of this endemism is warranted.

Cyanobacteria accounted for only 4% of the total *nifH* gene reads in our samples and dominated (>90% of total relative abundance) community composition in three samples from 25 m depth (two in the FZ, one in the WSC; Fig. 4). This contrasts with the Pacific sector of the AO, where Cyanobacteria dominate the diazotroph community, especially the nitroplast [107] of *Braarudosphaera bigelowii* (*Candidatus* Atelocyanobacterium thalassa or UCYN-A) is prevalent and active [27, 28]. We did not find UCYN-A in our samples from the Fram Strait. A seasonal study in the same region (WSC) similarly reported no findings of UCYN-A except in coastal fjord water [22]. More recently, UCYN-A was sporadically found along the Atlantic gateway to the AO, but *nifH* expression was only detected at the sea ice edge north of Svalbard [75]. Hence, UCYN-A appears rare and is likely not a main contributor to nitrogen fixation in the Atlantic sector of the AO. Instead, most of the few cyanobacterial reads found were related to the order of *Nostocales*. These filamentous and heterocystous taxa are reported from, e.g., Arctic rivers and coastal environments [22], the Beaufort Sea [20], sea ice [82], and Greenland shelf waters [29]. They are also known from Arctic freshwater environments and glacial forefields [108, 109]. It is not known whether these taxa are active in marine waters, including the FZ and WSC of the Fram Strait, or whether they have been transported from rivers and/or with sea-ice floes or wind [82]. We acknowledge that diverse Cyanobacteria have been reported from the Fram Strait and Greenland Sea [29], however, this was likely due to the use of Cyanobacteria-specific primers. In conclusion, Cyanobacteria in the Fram Strait were few and not related to common oceanic diazotrophs.

Concluding Remarks

We have shown that nitrogen fixation rates in the Fram Strait range from undetectable to moderate (0–0.2 nmol N L^{-1} d^{-1}) in the southbound cold and CDOM-rich waters of EGC, to higher (0.31–10.15 nmol N L^{-1} d^{-1}) in the northbound and warm WSC associated with higher primary production. The most relatively abundant ASV (ASV1) was affiliated with the Beta-Arctic1 group, which showed the highest *nifH* gene abundance in the region with the highest nitrogen fixation and primary production. We suggest that a linkage between nitrogen fixation and primary production is driven by DOM freshly released from phytoplankton and utilizable by NCDs. Furthermore, we found that temperature was positively correlated with nitrogen fixation and the abundance of ASV1 in our dataset, suggesting that temperature might play a significant role for nitrogen fixation in the Fram Strait. Locally, nitrogen fixation was potentially important, sustaining up to 16.9% ± 12.3% of concurrent primary production in the EGC, but only up to 5.3% ± 6.7% in the WSC. More elaborate future studies are needed to substantiate our findings, given that increased Atlantification is predicted to enhance primary production in the WSC and potentially increase concurrent nitrogen fixation in the future. These insights are important for the prediction of primary production in the AO because nitrogen is a key determinant of primary production in the region, now and in the future [7, 12, 110].

Supplementary Information The online version contains supplementary material available at https://doi.org/10.1007/s00248-025-02673-3.

Acknowledgements We thank the captain and crew of the R/V *Kronprins Haakon*, as well as the science crew onboard for their support. Particularly, we thank Laura de Steur (Norwegian Polar Institute) for leading the science program, Paul Dodd (Norwegian Polar Institute) for coordinating the CTD measurements and sampling, and Colin A. Stedmon (Technical University of Denmark) for measuring inorganic nutrients. Finally, we thank two anonymous reviewers for their constructive advice on the manuscript.

Author Contributions SZ, LWvF and LR designed the study. SZ and RG-A collected samples. SZ performed molecular laboratory analyses and RG-A measured CDOM samples. SZ conducted data analyses of all data with help from LWvF. LWvF and OG conducted IRMS and MIMS analyses with guidance from MB. MAG assisted with ancillary data analyses. SZ and LR drafted the manuscript. All authors edited the manuscript and approved the final version.

Funding This work was supported by the Danish Council for Independent Research [6108-00013] and Independent Research Fund Denmark [2032-00001B] to LR. MB was partly funded by the BIOPOLE National Capability Multicenter Round 2 funding from the Natural Environment Research Council [NE/W004933/1]. The MIMS equipment used in this study was obtained with European FEDER Funds. LvF was funded by an Elite PhD scholarship grant from the Department of Biology, University of Copenhagen. RG-A was supported by the

Independent Research Fund Denmark [4251-00058B]. The ship time leading to these results was funded by the European Union H2020 as part of the EU Project ARICE [730965]. We extend our gratitude to the Norwegian Polar Institute for their support and resources in the sampling campaign, which have been instrumental in this research.

Data Availability Sequences are deposited in the National Centre for Biotechnology Information (NCBI) Sequence Read Archive (SRA) under reference number PRJNA1226117.

Declarations

Competing Interests The authors declare no competing interests.

References

1. Bates NR, Mathis JT (2009) The Arctic ocean marine carbon cycle: evaluation of air-sea CO_2 exchanges, ocean acidification impacts and potential feedbacks. Biogeosciences Discuss 6:2433–2459
2. Manizza M, Menemenlis D, Zhang H et al (2019) Modeling the recent changes in the Arctic Ocean CO<Subscript>2</Subscript>sink (2006–2013). Glob Biogeochem Cycles 33(3):420–438
3. Serreze MC, Francis JA (2006) The Arctic amplification debate. Clim Change 76:241–264
4. Rantanen M, Karpechko AYu, Lipponen A et al (2022) The Arctic has warmed nearly four times faster than the globe since 1979. Commun Earth Environ 3:168
5. Stroeve J, Notz D (2018) Changing state of Arctic sea ice across all seasons. Environ Res Lett 13:103001
6. Arrigo KR, Van Dijken GL (2015) Continued increases in Arctic Ocean primary production. Prog Oceanogr 136:60–70
7. Lewis KM, van Dijken GL, Arrigo KR (2020) Changes in phytoplankton concentration now drive increased Arctic Ocean primary production. Science 369:198–202
8. Ardyna M, Arrigo KR (2020) Phytoplankton dynamics in a changing Arctic ocean. Nat Clim Change 10:892–903
9. Sandven H, Granskog MA, Opdal AF et al (2025) Increased light availability in the Northern Barents Sea driven by sea ice loss. J Geophys Res Oceans 130:e2025JC022370
10. Mills MM, Brown ZW, Laney SR et al (2018) Nitrogen limitation of the summer phytoplankton and heterotrophic prokaryote communities in the Chukchi Sea. Front Mar Sci 5:362
11. Sejr MK, Bruhn A, Dalsgaard T et al (2022) Glacial meltwater determines the balance between autotrophic and heterotrophic processes in a Greenland fjord. Proc Natl Acad Sci U S A 119:e2207024119
12. Tremblay J-É, Gagnon J (2009) The effects of irradiance and nutrient supply on the productivity of Arctic waters: a perspective on climate change. In: Nihoul JCJ, Kostianoy AG (eds) Influence of Climate Change on the Changing Arctic and Sub-Arctic Conditions. Springer Netherlands, Dordrecht, pp 73–93
13. Årthun M, Eldevik T, Smedsrud LH et al (2012) Quantifying the influence of Atlantic heat on Barents Sea Ice Variability and Retreat . J Clim 25:4736–4743
14. Ingvaldsen RB, Assmann KM, Primicerio R et al (2021) Physical manifestations and ecological implications of Arctic atlantification. Nat Rev Earth Environ 2:874–889
15. Postgate JR (1970) Biological nitrogen fixation. Nature 226:25–27
16. Karl D, Letelier R, Tupas L et al (1997) The role of nitrogen fixation in biogeochemical cycling in the subtropical North Pacific ocean. Nature 388:533–538
17. Capone DG, Burns JA, Montoya JP et al (2005) Nitrogen fixation by *Trichodesmium* spp.: an important source of new nitrogen to the tropical and subtropical North Atlantic Ocean. Glob Biogeochem Cycles 19:GB2024
18. von Friesen LW, Riemann L (2020) Nitrogen fixation in a changing Arctic ocean: an overlooked source of nitrogen? Front Microbiol 11:596426
19. Zehr JP, Mellon MT, Zani S (1998) New nitrogen-fixing microorganisms detected in oligotrophic oceans by amplification of nitrogenase (*nifH*) genes. Appl Environ Microbiol 64:3444–3450
20. Blais M, Tremblay J, Jungblut AD et al (2012) Nitrogen fixation and identification of potential diazotrophs in the Canadian Arctic. Glob Biogeochem Cycles 26:2011GB004096
21. Shiozaki T, Fujiwara A, Ijichi M et al (2018) Diazotroph community structure and the role of nitrogen fixation in the nitrogen cycle in the Chukchi Sea (western Arctic Ocean). Limnol Oceanogr 63:2191–2205
22. von Friesen LW, Paulsen ML, Müller O et al (2023) Glacial meltwater and seasonality influence community composition of diazotrophs in Arctic coastal and open waters. FEMS Microbiol Ecol 99:fiad067
23. Robicheau BM, Tolman J, Rose S et al (2023) Marine nitrogen-fixers in the Canadian Arctic Gateway are dominated by biogeographically distinct noncyanobacterial communities. FEMS Microbiol Ecol 99:fiad122
24. Capone DG, Zehr JP, Paerl HW et al (1997) *Trichodesmium*, a globally significant marine cyanobacterium. Science 276:1221–1229
25. Moisander PH, Beinart RA, Voss M et al (2008) Diversity and abundance of diazotrophic microorganisms in the South China Sea during intermonsoon. ISME J 2:954–967
26. Hallstrøm S, Benavides M, Salamon ER et al (2022) Activity and distribution of diazotrophic communities across the cape Verde frontal zone in the Northeast Atlantic ocean. Biogeochemistry 160:49–67
27. Shiozaki T, Bombar D, Riemann L et al (2017) Basin scale variability of active diazotrophs and nitrogen fixation in the North Pacific, from the tropics to the subarctic Bering Sea. Glob Biogeochem Cycles 31:996–1009
28. Harding K, Turk-Kubo KA, Sipler RE et al (2018) Symbiotic unicellular cyanobacteria fix nitrogen in the Arctic Ocean. Proc Natl Acad Sci USA 115:13371–13375
29. Díez B, Bergman B, Pedrós-Alió C et al (2012) High cyanobacterial *nif* H gene diversity in Arctic seawater and sea ice brine. Environ Microbiol Rep 4:360–366
30. Sipler RE, Gong D, Baer SE et al (2017) Preliminary estimates of the contribution of Arctic nitrogen fixation to the global nitrogen budget. Limnol Oceanogr Lett 2:159–166

31. Benavides M, Voss M (2015) Five decades of N_2 fixation research in the North Atlantic Ocean. Front Mar Sci 2:40
32. Rudels B, Carmack E (2022) Arctic ocean water mass structure and circulation. Oceanography 35:52–65
33. Haine TWN, Curry B, Gerdes R et al (2015) Arctic freshwater export: status, mechanisms, and prospects. Glob Planet Change 125:13–35
34. Swift JH, Aagaard K (1981) Seasonal transitions and water mass formation in the Iceland and Greenland seas. Deep Sea Res Part Oceanogr Res Pap 28:1107–1129
35. Cabedo-Sanz P, Belt ST (2016) Seasonal sea ice variability in eastern Fram Strait over the last 2000 years. Arktos 2:22
36. Dodd PA, Rabe B, Hansen E et al (2012) The freshwater composition of the Fram Strait outflow derived from a decade of tracer measurements. J Geophys Res Oceans 117:C11005
37. Gonçalves-Araujo R, Granskog MA, Bracher A et al (2016) Using fluorescent dissolved organic matter to trace and distinguish the origin of Arctic surface waters. Sci Rep 6:33978
38. Torres-Valdés S, Tsubouchi T, Bacon S et al (2013) Export of nutrients from the Arctic Ocean. J Geophys Res Oceans 118:1625–1644
39. Pavlov AK, Granskog MA, Stedmon CA et al (2015) Contrasting optical properties of surface waters across the Fram Strait and its potential biological implications. J Mar Syst 143:62–72
40. Fadeev E, Salter I, Schourup-Kristensen V et al (2018) Microbial communities in the East and West Fram Strait during sea ice melting season. Front Mar Sci 5:429
41. Krisch S, Browning TJ, Graeve M et al (2020) The influence of Arctic Fe and Atlantic fixed N on summertime primary production in Fram Strait, North Greenland sea. Sci Rep 10:15230
42. Wietz M, Engel A, Ramondenc S et al (2024) The Arctic summer microbiome across Fram Strait: depth, longitude, and substrate concentrations structure microbial diversity in the euphotic zone. Environ Microbiol 26:e16568
43. Engel A, Bracher A, Dinter T et al (2019) Inter-annual variability of organic carbon concentration in the Eastern Fram Strait during summer (2009–2017). Front Mar Sci 6:187
44. Gonçalves-Araujo R, Stedmon CA, De Steur L et al (2020) A Decade of Annual Arctic DOC Export With Polar Surface Water in the East Greenland Current. *Geophys Res Lett* ; 47: e2020GL089686
45. Hansen HP, Koroleff F (1999) Determination of nutrients. Methods Seawater Anal 159–228
46. Schnetger B, Lehners C (2014) Determination of nitrate plus nitrite in small volume marine water samples using vanadium(III) chloride as a reduction agent. Mar Chem 160:91–98
47. Redfield AC (1934) On the proportions of organic derivatives in sea water and their relation to the composition of plankton. *Univ Press Liverp* ; st
48. Schlitzer R (2023) Ocean Data View v.5.8.1
49. Vihtakari M (2022) GgOceanMaps: plot data in oceanographic maps using ggplot2. ; v.1.3.4. https://mikkovihtakari.github.io/ggOceanMaps/
50. Stedmon CA, Markager S (2001) The optics of chromophoric dissolved organic matter (CDOM) in the Greenland sea: an algorithm for differentiation between marine and terrestrially derived organic matter. Limnol Oceanogr 46:2087–2093
51. Klawonn I, Lavik G, Böning P et al (2015) Simple approach for the preparation of 15 – 15N2-enriched water for nitrogen fixation assessments: evaluation, application and recommendations. Front Microbiol 6:769
52. Stöven T, Tanhua T, Hoppema M et al (2016) Transient tracer distributions in the Fram Strait in 2012 and inferred anthropogenic carbon content and transport. Ocean Sci 12:319–333
53. Kana TM, Darkangelo Christina H, MDuane et al (1994) Membrane Inlet mass spectrometer for rapid High-Precision determination of N2, O2, and ar in environmental water samples. Anal Chem 66:4166–4170
54. Benavides M, Martias C, Elifantz H et al (2018) Dissolved organic matter influences N_2 fixation in the New Caledonian Lagoon (Western Tropical South Pacific). Front Mar Sci 5:89
55. Montoya JP, Voss M, Ahler PK et al (1996) A Simple, High-Precision, High-Sensitivity tracer assay for N2 fixation. Appl Environ Microbiol 62:986–993
56. White AE, Granger J, Selden C et al (2020) A critical review of the $^{15}N_2$ tracer method to measure diazotrophic production in pelagic ecosystems. Limnol Oceanogr Methods 18:129–147
57. Gradoville MR, Bombar D, Crump BC et al (2017) Diversity and activity of nitrogen-fixing communities across ocean basins. Limnol Oceanogr 62:1895–1909
58. Hama T, Hama J, Handa N (1993) 13 C tracer methodology in microbial ecology with special reference to primary production processes in aquatic environments. Adv Microb Ecol 13:39–83
59. Martiny AC, Pham CTA, Primeau FW et al (2013) Strong latitudinal patterns in the elemental ratios of marine plankton and organic matter. Nat Geosci 6:279–283
60. Zehr JP, Turner PJ Nitrogen fixation: nitrogenase genes and gene expression. Methods Microbiol 30:271–286
61. Zani S, Mellon MT, Collier JL et al (2000) Expression of *nifH* genes in natural microbial assemblages in Lake George, New York, detected by reverse transcriptase PCR. Appl Environ Microbiol 66:3119–3124
62. Zehr JP, McReynolds LA (1989) Use of degenerate oligonucleotides for amplification of the NifH gene from the marine Cyanobacterium *richodesmium thiebautii*. Appl Environ Microbiol 55:2522–2526
63. Callahan BJ, McMurdie PJ, Rosen MJ et al (2016) DADA2: high-resolution sample inference from illumina amplicon data. Nat Methods 13:581–583
64. Angel R, Nepel M, Panhölzl C et al (2018) Evaluation of primers targeting the Diazotroph functional gene and development of NifMAP – a bioinformatics pipeline for analyzing NifH amplicon data. Front Microbiol 9:703
65. Frank IE, Turk-Kubo KA, Zehr JP (2016) Rapid annotation of nif<Emphasis Type="ItalicSmallCaps">H</Emphasis>gene sequences using classification and regression trees facilitates environmental functional gene analysis. Environ Microbiol Rep 8:905–916
66. Moynihan MA, Furbo Reeder C (2023) nifHdada2 Github Repository. ; 7996213
67. Heller P, Tripp HJ, Turk-Kubo K et al (2014) ARBitrator: a software pipeline for on-demand retrieval of auto-curated*nifH*sequences from GenBank. Bioinformatics 30:2883–2890
68. Davis NM, Proctor DM, Holmes SP et al (2018) Simple statistical identification and removal of contaminant sequences in marker-gene and metagenomics data. Microbiome 6:226
69. Rstudio Team RStudio: Integrated Development Environment for R
70. McMurdie PJ, Holmes S (2013) Phyloseq: an R package for reproducible interactive analysis and graphics of microbiome census data. PLoS ONE 8:e61217
71. Oksanen J, Simpson G, Blanchet FG et al (2022) Vegan community ecology package version *2:6-2 April 2022*
72. Katoh K, Standley DM (2013) MAFFT multiple sequence alignment software version 7: improvements in performance and usability. Mol Biol Evol 30:772–780
73. Edler D, Klein J, Antonelli A et al (2021) RaxmlGUI 2.0: a graphical interface and toolkit for phylogenetic analyses using RAxML. Methods Ecol Evol 12:373–377
74. Letunic I, Bork P (2021) Interactive tree of life (iTOL) v5: an online tool for phylogenetic tree display and annotation. Nucleic Acids Res 49:W293–W296

75. von Friesen LW, Laber CP, Kristensen BH et al (2025) From temperate to Polar waters: transition to non-cyanobacterial diazotrophy upon entering the Atlantic gateway of the Arctic ocean. Limnol Oceanogr 9999:1–17
76. Armbruster DA, Pry T (2008) Limit of blank, limit of detection and limit of quantitation. Clin Biochem Rev 29:49–52
77. Van Den Boogaart KG, Tolosana-Delgado R (2008) Compositions": a unified R package to analyze compositional data. Comput Geosci 34:320–338
78. Martinez Arbizu P, PairwiseAdonis: Pairwise multilevel comparison using adonis. R Package Version 04
79. Wickham H (2016) ggplot2. ; v.3.4.0.
80. Barnett D, Arts I, Penders J (2021) MicroViz: an R package for microbiome data visualization and statistics. J Open Source Softw 6:3201
81. Dahl EM, Neer E, Bowie KR et al (2022) Microshades: an R package for improving color accessibility and organization of microbiome data. Microbiol Resour Announc. https://doi.org/10.1128/mra.00795-22
82. Fernández-Méndez M, Turk-Kubo KA, Buttigieg PL et al (2016) Diazotroph diversity in the sea ice, melt ponds, and surface waters of the Eurasian basin of the central Arctic Ocean. Front Microbiol 7:1884
83. Chien YT, Zinder SH (1996) Cloning, functional organization, transcript studies, and phylogenetic analysis of the complete nitrogenase structural genes (nifHDK2) and associated genes in the archaeon *methanosarcina barkeri* 227. J Bacteriol 178:143–148
84. Randelhoff A, Reigstad M, Chierici M et al (2018) Seasonality of the physical and biogeochemical hydrography in the inflow to the Arctic Ocean through Fram Strait. Front Mar Sci 5:224
85. Tuerena RE, Hopkins J, Buchanan PJ et al (2021) An Arctic strait of two halves: the changing dynamics of nutrient uptake and limitation across the Fram Strait. Glob Biogeochem Cycles 35:e2021GB006961
86. Jørgensen L, Stedmon CA, Granskog MA et al (2014) Tracing the long-term microbial production of recalcitrant fluorescent dissolved organic matter in seawater. Geophys Res Lett 41:2481–2488
87. Filella A, Cébron A, Paix B et al (2025) Organic metabolite uptake by diazotrophs in the North Pacific Ocean. ISME Commun 5:ycaf061
88. Breitbarth E, Oschlies A, LaRoche J (2007) Physiological constraints on the global distribution of *Trichodesmium* – effect of temperature on diazotrophy. Biogeosciences 4:53–61
89. Stal LJ (2009) Is the distribution of nitrogen-fixing cyanobacteria in the oceans related to temperature? Environ Microbiol 11:1632–1645
90. Zehr JP, Capone DG (2021) Marine nitrogen fixation. Springer Int Publ ; 95–115
91. Chakraborty S, Andersen KH, Merico A et al (2025) Particle-associated N_2 fixation by heterotrophic bacteria in the global ocean. Sci Adv 11:eadq4693
92. von Friesen LW, Farnelid H, von Appen W-J et al (2025) Nitrogen fixation under declining Arctic sea ice. Commun Earth Environ 6:811
93. Hop H, Falk-Petersen S, Svendsen H et al (2006) Physical and biological characteristics of the pelagic system across Fram Strait to Kongsfjorden. Prog Oceanogr 71:182–231
94. Nöthig E-M, Bracher A, Engel A et al (2015) Summertime plankton ecology in Fram Strait—a compilation of long- and short-term observations. Polar Res 34:23349
95. von Jackowski A, Grosse J, Nöthig E-M et al (2020) Dynamics of organic matter and bacterial activity in the Fram Strait during summer and autumn. Philos Trans R Soc Lond A Math Phys Eng Sci 378:20190366
96. Benavides M, Moisander PH, Berthelot H et al (2015) Mesopelagic N2 fixation related to organic matter composition in the Solomon and Bismarck seas (Southwest Pacific). PLoS One 10:e0143775
97. Benavides M, Duhamel S, Van Wambeke F et al (2020) Dissolved organic matter stimulates N2 fixation and *nifH* gene expression in *Trichodesmium*. FEMS Microbiol Lett 367:fnaa034
98. Filella A, Riemann L, Van Wambeke F et al (2022) Contrasting roles of DOP as a source of phosphorus and energy for marine diazotrophs. Front Mar Sci 9:923765
99. Bombar D, Paerl RW, Riemann L (2016) Marine non-cyanobacterial diazotrophs: moving beyond molecular detection. Trends Microbiol 24:916–927
100. Granskog MA, Stedmon CA, Dodd PA et al (2012) Characteristics of colored dissolved organic matter (CDOM) in the Arctic outflow in the Fram Strait: assessing the changes and fate of terrigenous CDOM in the Arctic Ocean. J Geophys Res Oceans 117:C12021
101. Knapp AN (2012) The sensitivity of marine N2 fixation to dissolved inorganic nitrogen. Front Microbiol 3:374
102. Salinero K, Keller K, Feil WS et al (2009) Metabolic analysis of the soil microbe *Dechloromonas aromatica* str. RCB: indications of a surprisingly complex life-style and cryptic anaerobic pathways for aromatic degradation. BMC Genomics 10:351
103. Tschitschko B, Esti M, Philippi M et al (2024) Rhizobia–diatom symbiosis fixes missing nitrogen in the ocean. Nature 630:899–904
104. Turk-Kubo KA, Gradoville MR, Cheung S et al (2023) Non-cyanobacterial diazotrophs: global diversity, distribution, ecophysiology, and activity in marine waters. FEMS Microbiol Rev 47:fuac046
105. Farnelid H, Andersson AF, Bertilsson S et al (2011) Nitrogenase gene amplicons from global marine surface waters are dominated by genes of non-cyanobacteria. PLoS One 6:e19223
106. Shiozaki T, Nishimura Y, Yoshizawa S et al (2023) Distribution and survival strategies of endemic and cosmopolitan diazotrophs in the Arctic Ocean. ISME J 17:1340–1350
107. Coale TH, Loconte V, Turk-Kubo KA et al (2024) Nitrogen-fixing organelle in a marine alga. Science 384:217–222
108. Jungblut AD, Lovejoy C, Vincent WF (2010) Global distribution of cyanobacterial ecotypes in the cold biosphere. ISME J 4:191–202
109. Nash MV, Anesio AM, Barker G et al (2018) Metagenomic insights into diazotrophic communities across Arctic glacier forefields. FEMS Microbiol Ecol 94:fiy114
110. Slagstad D, Wassmann PFJ, Ellingsen I (2015) Physical constrains and productivity in the future Arctic Ocean. Front Mar Sci 2:85